



Original Article

# Synthesis of TiO<sub>2</sub> Nanotubes for Improving the Corrosion Resistance Performance of the Titanium Implants

Duong Hong Quan<sup>1</sup>, Nguyen Viet Tung<sup>1,2</sup>, Ta Quoc Tuan<sup>1</sup>, Le Thi Tam<sup>1</sup>,  
Pham Thi Mai Phuong<sup>1</sup>, Cao Xuan Thang<sup>1</sup>, Dao Xuan Viet<sup>1</sup>, Nguyen Kien Trung<sup>1</sup>,  
Pham Van Huan<sup>1</sup>, Nguyen Thi Ngoc<sup>1</sup>, Tran Trong An<sup>1,\*</sup>, Pham Hung Vuong<sup>1</sup>

<sup>1</sup>Hanoi University of Science and Technology (HUST), 01 Dai Co Viet, Hanoi, Vietnam

<sup>2</sup>Institute of Science and Technology, Ministry of Public Security,  
47 Pham Van Dong, Hanoi, Vietnam

Received 11 May 2022

Revised 06 July 2022; Accepted 27 July 2022

**Abstract:** TiO<sub>2</sub> nanotubes were successfully synthesized by electrochemical method. A fluoride salt mixture was used as an electrolyte for synthesizing TiO<sub>2</sub> nanotubes on titanium substrates. In this work, we have reported the synthesis procedure of TiO<sub>2</sub> nanotubes and investigated the corrosion resistance of TiO<sub>2</sub> nanotubes coated on the Ti substrate. FE-SEM was used to observe the morphology and determine the size of the TiO<sub>2</sub> nanotubes. The phase formation and crystal quality of TiO<sub>2</sub> nanotubes were studied by XRD measurements. One-microliter distilled water droplets were used to define the wettability of the TiO<sub>2</sub> nanotube surfaces by measuring the contact angle. The corrosion resistance behavior of specimens was analyzed in the simulated body fluid solution (SBF) using potentiodynamic polarization tests for potential application as implants.

**Keywords:** TiO<sub>2</sub> nanotubes, corrosion resistance, titanium, implants.

## 1. Introduction

Titanium and its alloys have been extensively utilized as implant materials in the biomedical field thanks to their mechanical and chemical features such as excellent fatigue and tensile strength, superior corrosion and wear resistance, low modulus of elasticity, good hardness, low density, and especially, they are not cytotoxic when they bonded to bone and surrounding tissues [1, 2]. Their

\* Corresponding author.

E-mail address: [an.trantrong@hust.edu.vn](mailto:an.trantrong@hust.edu.vn)

<https://doi.org/10.25073/2588-1124/vnumap.4732>

biocompatibility is due to the formation of an oxide film on the surface of the material. The 1.5 to 10 nm-thick films are chemically stable. They can be formed by exposure to the air or moisture at room temperature, protecting these material surfaces from environmental influences [3]. However, this oxide layer was limited due to low surface hardness, wear resistance, and a high coefficient of friction, so they are easily dissolved, when put into the human body [4]. This dissolution of titanium substances into the human body not only adversely affects bone and surrounding tissue healing but also enhances cytokines release, sometimes leading to acute coating or chronic effects [5, 6]. Therefore, the improvement of the corrosion resistance of the coating has been of significant research interest. In this work, we have developed TiO<sub>2</sub> nanotube coatings formed on Ti substrate by electrochemical method. The research results show that the outermost TiO<sub>2</sub> nanotubes can directly bond with titanium substrate with excellent corrosion resistance which can effectively inhibit the dissolution of Ti into the human body, strongly increasing the adhesion strength. The electrochemical method provides simple and inexpensive routes for the synthesis of ceramic thin films and coatings [7]. Therefore, the aim of the work is to investigate the effect of TiO<sub>2</sub> nanotube formation on corrosion resistance properties in simulated body fluid (SBF) for potential application in implants.

## 2. Experimental Procedure

The commercial titanium plates (10 × 10 × 0.1 mm<sup>3</sup>, Merck, 99.9 %) were used for substrates. The Ti plates were first washed ultrasonically with acetone for about 20 min, then completely washed with redistilled water, and finally dried in a vacuum oven at 40 °C for 2 h. Ti plates are used as Ti electrodes after completely washing. The electrolytes of the electrochemical method were prepared using ammonium fluoride (NH<sub>4</sub>F, Sigma, 99.9 %), ethylene glycol solution (C<sub>2</sub>H<sub>6</sub>O<sub>2</sub>- Sigma, 99.9 %), and H<sub>2</sub>O. The electrochemical process was carried out at 50 voltages for 1 h using a DC power supply. Later, the TiO<sub>2</sub> layer was followed by heat treatment at 550 °C for 2 h.

The microstructure was determined by field emission scanning electron microscopy FE-SEM (JEOL, JSM-6700F, JEOL Techniques, Tokyo, Japan). The crystalline structures of the TiO<sub>2</sub> nanotubes were characterized by X-ray diffraction (XRD, D8 Advance, Bruker, Germany). One-microliter distilled water droplets were used to define the wettability of the TiO<sub>2</sub> nanotube surfaces by measuring the contact angle. Simulated body fluid (SBF) (SBF: 8.035 g NaCl; 0.355 g NaHCO<sub>3</sub>; 0.225 g KCl; 0.231 g K<sub>2</sub>HPO<sub>4</sub>·3H<sub>2</sub>O; 0.311 g MgCl<sub>2</sub>·6H<sub>2</sub>O; 0.292 g CaCl<sub>2</sub>; 0.072 g Na<sub>2</sub>SO<sub>4</sub>; 6.118 g ((HOCH<sub>2</sub>)<sub>3</sub>CNH<sub>2</sub> and HCl with an appropriate amount for adjusting the pH ~ 7.4 [8]) was used as the biological electrolyte for the corrosion test. Potentiodynamic polarization tests were carried out by suspending the samples in SBF solution (pH ≈ 7) at room temperature (298K) at a scan rate of 2 mV·s<sup>-1</sup> from -300 to 300 mV using a Zahner Zennium electrochemical workstation. The corrosion potential (E<sub>corr</sub>), corrosion current density (i<sub>corr</sub>), and polarization resistance (R<sub>corr</sub>) were determined using the Tafel extrapolation method [9, 10]:

$$R_{corr} = \frac{\beta_a \beta_b}{2.303 i_{corr} (\beta_a + \beta_b)} \quad (1)$$

where  $\beta_a$  and  $\beta_b$  are the anodic and cathodic Tafel slope of the sample.

The corrosion rate (C.R) can be determined from the corrosion current density using Faraday's law [11, 12]:

$$C.R = \frac{M}{nF\rho} i_{corr} = 3.73 \times 10^{-4} \frac{M}{n\rho} i_{corr} \text{ (g/m}^2\text{h)} \quad (2)$$

where M is the atomic weight of the metal,  $\rho$  is the density, n is the number of electrons transferred per metal atom and F is the Faraday constant (F= 96.485 C/mol).

### 3. Results and Discussions

The electrochemical method often leads to poorly ordered products making unequivocal structural characterization difficult and the product comes with X-ray amorphous impurities, although occasionally crystalline features are observed [6]. Therefore, high-temperature annealing is necessary to convert amorphous to crystalline forms [13].

The XRD patterns of the bare Ti and the TiO<sub>2</sub> nanotubes on Ti substrate fabricated by the electrochemical method after heat treatment at 550 °C are displayed in Figure 1. The coating primarily consisted of the anatase phase, while the peak of the rutile phase was also detected in the XRD pattern of the TiO<sub>2</sub> nanotube sample. In addition to the characteristic peaks of Ti (JCPDS 44-1294), the synthesized TiO<sub>2</sub> nanotubes showed a relatively strong peak at  $2\theta \sim 25.7^\circ$ ;  $38.3^\circ$ ;  $48.64^\circ$ ;  $54.37^\circ$  corresponding to the (101) (112) (200) (105). All of the peaks can be indexed to the crystalline TiO<sub>2</sub> (anatase) structure (JCPDS 21-1272). Peak was located at  $56.4^\circ$  along with miller indices value (220) in agreement with TiO<sub>2</sub> (rutile) structure (JCPDS 21-1276) [14]. Based on these findings, the TiO<sub>2</sub> nanotubes on the Ti substrates were synthesized successfully.

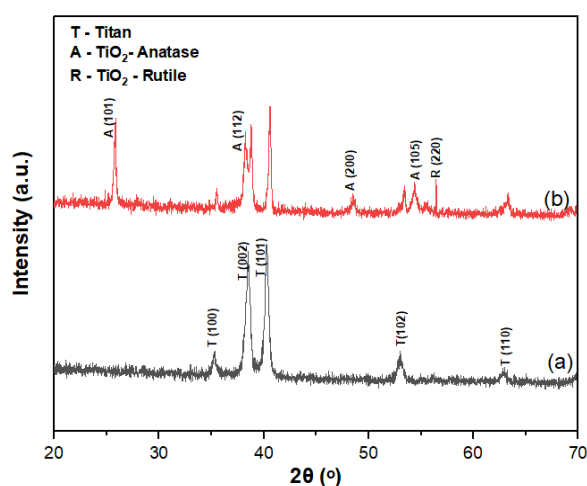


Figure 1. XRD patterns of Ti (a) and TiO<sub>2</sub> nanotubes (b) on Ti substrate after heat treatment at 550 °C for 2 h.

The electrochemical method on Ti substrate forms a structure of TiO<sub>2</sub> nanotubes. This has been proven in many previous publications [15-16]. At the beginning of the electrochemical process, amorphous TiO<sub>x</sub> formed on the Ti substrates by contact with the electrolyte solution [17].



Meanwhile, ionization of electrolyte components including fluoride salt and water can lead to the formation of F<sup>-</sup>, H<sup>+</sup> and OH<sup>-</sup>, respectively. Such ions may also lead to the formation and growth of the TiO<sub>2</sub> layer. The proposed reaction mechanism through the following reactions [18, 19]:

At anode:



At cathode:



The reactions are following:



The formation (8) and the dissolution (9) of  $\text{TiO}_2$  that happened continuously is the basis for the porous structure of the  $\text{TiO}_2$  nanotube layer. In the electrolyte solution, the presence of  $\text{Ti}^{4+}$  led to the adsorption of the  $[\text{TiF}_6]^{2-}$  ions on the oxide surface, decreasing the surface energy, and increasing surface perturbation.

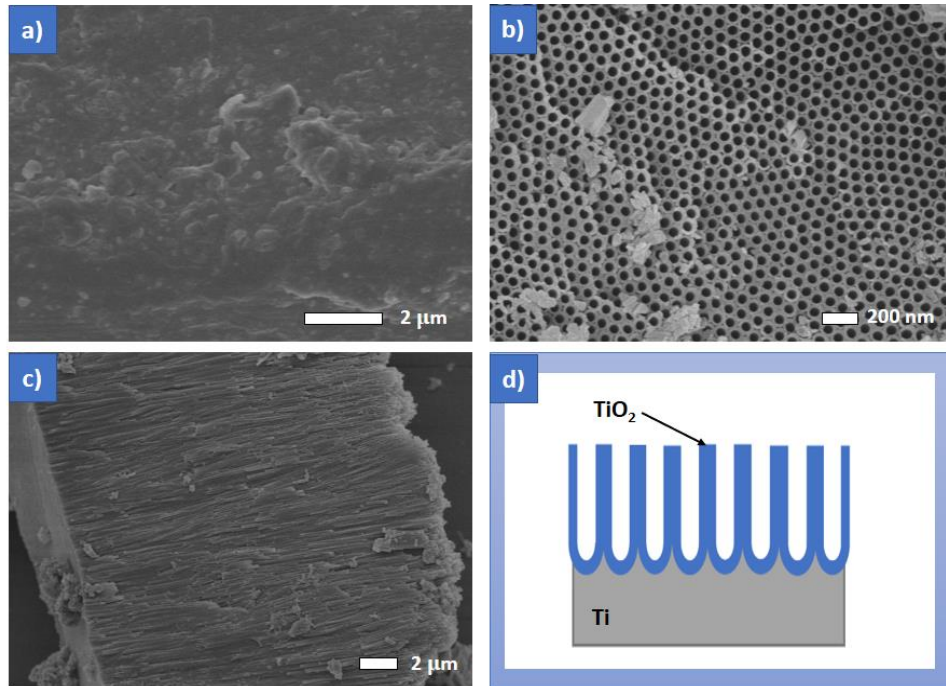


Figure 2. FE-SEM images of Ti (a),  $\text{TiO}_2$  nanotubes (b, c), and schematic of the formation of the  $\text{TiO}_2$  nanotubes on Ti substrates (d).

The  $\text{TiO}_2$  nanotube growth morphology was observed by FE-SEM. The coating layer appeared to be highly dense and uniform, with an average inner diameter of 70 nm and outer diameter of 140 nm (Figure 2b). The thicknesses of the  $\text{TiO}_2$  layers were approximately of 16  $\mu\text{m}$  (Figure 2c). Wang et al., studied the effects of  $\text{TiO}_2$  nanotubes with different diameters of 30 nm, 70 nm and 100 nm on biological bone responses around the implants [20]. They found that 70 nm in diameter is the optimum size for  $\text{TiO}_2$  nanotube coated on titanium implants to obtain favorable osseointegration. The model of the  $\text{TiO}_2$  nanotube structure formed on the Ti substrate is built as shown in Figure 2d.

The contact angle, which tends to decrease as the roughness increases for  $\text{TiO}_2$  nanotubes, represents the degree of hydrophilicity. The shape of water drops on the titanium and  $\text{TiO}_2$  nanotube surfaces is presented in Figure 3. The results showed that anodizing of titanium increased the hydrophilicity of the titanium surface. This might be because of the increase in the surface roughness, as above mentioned. The surface wettability of biomaterials has been found to be an important factor for cell-biomaterial interaction and more hydrophilic surfaces are able to improve cellular properties [21].

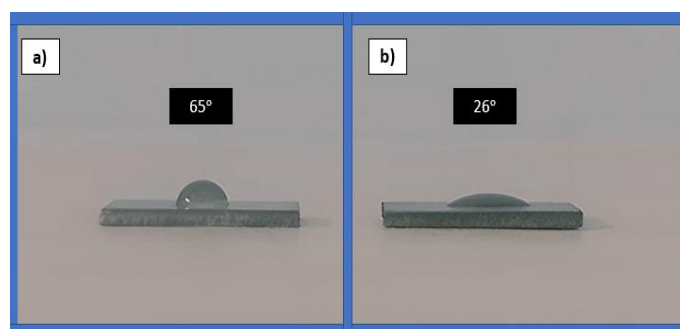


Figure 3. Measurement of wettability of Ti (a) and TiO<sub>2</sub> nanotubes (b).

The free corrosion potential (FCP) plots and potentiodynamic polarization curves of the bare Ti substrate and TiO<sub>2</sub> nanotubes on the Ti substrate are shown in Figure 4. The extracted parameters from the polarization plots including the corrosion potential ( $E_{\text{corr}}$ ) and corrosion current density ( $i_{\text{corr}}$ ) are given in Table 1.

Table 1. The results of corrosion parameters

Sample	$E_{\text{corr}}$ (V)	$i_{\text{corr}} \times 10^{-7}$ (A/cm <sup>2</sup> )	$\beta a$ (V)	$\beta c$ (V)	$R_{\text{corr}}$ (k $\Omega$ )	Corrosion rate (mg/m <sup>2</sup> h)
Ti	-0.608	0.217	0.1482	0.2706	1916	0.971
TiO <sub>2</sub> nanotubes	-0.411	0.050	0.0740	0.1029	3738	0.224

Potentiostatic polarization experiments used to observe anodic and cathodic behaviors allow the controlled polarization of a metal surface in an electrolyte [22]. Measurements of the current vs time relationship under a constant applied potential are obtained from the experiment. Cathode polarization: the potential shifts in the negative direction (below  $E_{\text{corr}}$ ), and the electrons accumulate in the metal surface and forcing the working electrode to become more negative. Anode polarization: the potential is changed in the anodic (on  $E_{\text{corr}}$ ) causing the electrons to be removed from the metal surface and the working electrode to become the anode.

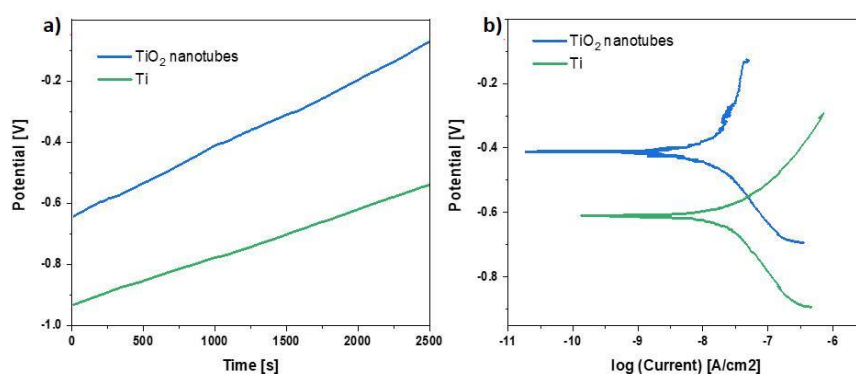


Figure 4. Free corrosion potential (a) and potentiodynamic polarization plots of Ti and TiO<sub>2</sub> nanotubes on Ti substrates (b).

The corrosion potential, corrosion current density (corrosion rate), and polarization resistance of the coatings were used to characterize the corrosion protective property of the coatings. The high corrosion potential, polarization resistance, and low corrosion current density (low corrosion rate) of the coatings suggested a high corrosion resistance performance [23]. Figure 4a demonstrated the free corrosion potential (FCP) as a function of time. The FCP increased with time, and it was almost 200 mV higher in the presence of TiO<sub>2</sub> nanotube coating. The rise of FCP values towards the positive direction indicates that on the investigated surface is formed a passive layer which indicates a better corrosion resistance, this was also confirmed by FE-SEM studies [24, 25], The rise in potential is the indication of the formation as well as thickening of the surface film with immersion time.

As shown in Figure 4b and Table 1, TiO<sub>2</sub> nanotube coatings on the Ti substrate was superior corrosion resistance compared to the bare Ti substrates, with a relatively low corrosion rate. While  $E_{\text{corr}}$  represents the thermodynamic tendency for corrosion,  $i_{\text{corr}}$  shows the corrosion rate [3]. The electrochemical samples observed the dynamic potential polarization graph tended to shift toward the region of the lower corrosion current density and the higher corrosion potential of the TiO<sub>2</sub> nanotube coating, confirming an improvement in the corrosion resistance [26]. The corrosion rate of titanium was found 0.971 (mg/m<sup>2</sup>h). TiO<sub>2</sub> nanotube layer formed outside, and the corrosion rate decreased to 0.224 (mg/m<sup>2</sup>h). This indicated that the electrochemical process significantly improved the corrosion resistance of the bare titanium.

#### 4. Conclusions

TiO<sub>2</sub> nanotubes formation on the Ti substrates has been synthesized successfully by the electrochemical process. The obtained TiO<sub>2</sub> nanotubes were of 70 nm in inner diameter and of approximately 16 μm in thickness. This coating exhibited higher hydrophilicity than that of the bare Ti substrates, which is attributed to better roughness and porosity. Compared with the bare Ti substrates, the presence of TiO<sub>2</sub> nanotube coatings increased the corrosion potential and clearly decreased its corrosion current density in the SBF solution, thus improving the corrosion resistance. These results suggest that the utility of a TiO<sub>2</sub> nanotubes coating opens up more opportunities for wide-range applications from medical implants to anticorrosive engineering materials after simple surface modification using electrochemical synthesis.

#### References

- [1] A. Krzakała, K. Służalska, G. Dercz, A. Maciej, A. Kazek, J. Szade, A. Winiarski, M. Dudek, J. Michalska, G. Tylko, A. M. Osyczka, W. Simka, Characterization of Bioactive Films on Ti–6Al–4V Alloy, *Electrochim. Acta*, Vol. 104, No. 1, 2013, pp. 425-438, <https://doi.org/10.1016/j.electacta.2012.12.081>.
- [2] K. Gulati, S. Ramakrishnan, M. S. Aw, G. J. Atkins, D. M. Findlay, D. Losic, Biocompatible Polymer Coating of Titania Nanotube Arrays for Improved Drug Elution and Osteoblast Adhesion, *Acta Biomater*, Vol. 8, No. 1, 2012, pp. 449-456, <https://doi.org/10.1016/j.actbio.2011.09.004>.
- [3] F. Alhosseini, M. K. Keshavarz, M. Molaei, S. O.Gashti, Plasma Electrolytic Oxidation (PEO) Process on Commercially Pure Ti Surface: Effects of Electrolyte on the Microstructure and Corrosion Behavior of Coatings, *Metall. Mater. Trans. A: Phys. Metall. Mater. Sci.*, Vol. 49, No. 10, pp. 4966-4979, <https://doi.org/10.1007/s11661-018-4824-8>.
- [4] M. Mu, J. Liang, X. Zhou, Q. Xiao, One-step Preparation of TiO<sub>2</sub>/MoS<sub>2</sub> Composite Coating on Ti6Al4V Alloy by Plasma Electrolytic Oxidation and its Tribological Properties, *Surf. Coat. Technol*, Vol. 214, No. 15, 2013, pp. 124-130, <https://doi.org/10.1016/j.surfcoat.2012.10.079>.

- [5] M. C. G. Alonso, L. Saldaña, G. Vallés, J. L. G. Carrasco, J. G. Cabrero, M. E. Martínez; E. G. Garay, L. Munuera, In Vitro Corrosion Behaviour and Osteoblast Response of Thermally Oxidised Ti6Al4V Alloy, *Biomaterials*, Vol. 24, No. 1, 2003, pp. 19-26, [https://doi.org/10.1016/S0142-9612\(02\)00237-5](https://doi.org/10.1016/S0142-9612(02)00237-5).
- [6] J. Hao, Y. Li, X. Wang, X. Zhang, B. Li, H. Li, L. Zhou, F. Yin, C. Liang, H. Wang, Corrosion Resistance and Biological Properties of A Micro-Nano Structured Ti Surface Consisting of TiO<sub>2</sub> and hydroxyapatite, *RSC Adv*, Vol. 7, No. 53, 2017, pp. 33285-33292.
- [7] G. H. A. Therese, P. V. Kamath, Electrochemical Synthesis of Metal Oxides and Hydroxides, *Chem. Mater*, Vol. 12, No. 5, 2000, pp. 1195-1204, <https://doi.org/10.1021/cm990447a>.
- [8] A. Srinivasan, N. Rajendran, Surface Characteristics, Corrosion Resistance and MG63 Osteoblast-Like Cells Attachment Behaviour of Nano SiO<sub>2</sub>-ZrO<sub>2</sub> Coated 316L Stainless Steel, *RSC Adv*, Vol. 5, No. 33, 2015, pp. 26007-26016, <https://doi.org/10.1039/C5RA01881A>.
- [9] D. Shen, H. Ma, C. Guo, J. Cai, G. Li, D. H. Q. Yang, Effect of Cerium and Lanthanum Additives on Plasma Electrolytic Oxidation of AZ31 Magnesium Alloy, *J. Rare Earths*, Vol. 31, No. 12, 2013, pp. 1208-1213, [https://doi.org/10.1016/S1002-0721\(12\)60428-1](https://doi.org/10.1016/S1002-0721(12)60428-1).
- [10] A. Samide, A. Ciuciu, C. Negri, Surface Analysis of Inhibitor Film Formed by Poly(Vinyl Alcohol) on Stainless Steel in Sodium Chloride Solution, *Port. Electrochimica Acta*, Vol. 28, No. 6, 2010, pp. 28, 385-396, <https://doi.org/10.4152/pea.201006385>.
- [11] Y. S. Choi, J. J. Shim, J. G. Kim, Corrosion Behavior of Low Alloy Steels Containing Cr, Co and W in Synthetic Potable Water, *Mater. Sci. Eng. A*, Vol. 385, No. 1-2, 2004, pp. 148-156, <https://doi.org/10.1016/j.msea.2004.06.024>.
- [12] J. Liu, B. Zhang, W. H. Qi, Y. G. Deng, R. D. K. Misra, Corrosion Response of Zinc Phosphate Conversion Coating on Steel Fibers for Concrete Applications, *J. Mater. Res. Technol*, Vol. 9, No. 3, 2020, pp. 5912-5921, <https://doi.org/10.1016/j.jmrt.2020.03.117>.
- [13] N. K. Allam, C. A. Grimes, Room Temperature One-step Polyol Synthesis of Anatase TiO<sub>2</sub> Nanotube Arrays: Photoelectrochemical Properties, *Langmuir*, Vol. 25, No. 13, 2009, pp. 7234-7240, <https://doi.org/10.1021/la9012747>.
- [14] K. M. Prabu, S. Perumal, Micro Strain and Morphological Studies of Anatase and Rutile Phase TiO<sub>2</sub> Nanocrystals Prepared via Sol-Gel and Solvothermal Method - A Comparative Study, *International Journal of Scientific Research in Science, Engineering and Technology IJSRSET*, Vol. 1, No. 4, 2015, pp. 299-304.
- [15] D. Regonini, C. R. Bowen, A. Jaroenworarluck, R. Stevens, A Review of Growth Mechanism, Structure and Crystallinity of Anodized TiO<sub>2</sub> Nanotubes, *Mater. Sci. Eng. R Rep*, Vol. 74, No. 12, 2013, pp. 377-406, <https://doi.org/10.1016/j.mser.2013.10.001>.
- [16] S. J. Sital, K. S. Raja, Self-ordering Dual-layered Honeycomb Nanotubular Titania: A Study in Formation Mechanisms, *RSC Adv*, Vol. 6, No. 15, 2016, pp. 11991-12002, <https://doi.org/10.1039/C5RA24667A>.
- [17] E. Ahounbar, S. M. M. Khoei, H. Omidvar, Characteristics of In-situ Synthesized Hydroxyapatite on TiO<sub>2</sub> Ceramic Via Plasma Electrolytic Oxidation, *Ceram. Int*, Vol. 45, No. 3, 2019, pp. 3118-3125, <https://doi.org/10.1016/j.ceramint.2018.10.206>.
- [18] J. M. Macak, H. Tsuchiya, A. Ghicov, K. Yasuda, R. Hahn, S. Bauer, P. Schmuki, TiO<sub>2</sub> Nanotubes: Self-organized Electrochemical Formation, Properties and Applications, *Curr. Opin. Solid State Mater. Sci*, Vol. 11, No. 1-2, 2007, pp. 3-18, <https://doi.org/10.1016/j.cossms.2007.08.004>.
- [19] P. Roy, S. Berger, P. Schmuki, TiO<sub>2</sub> Nanotubes: Synthesis and Applications, *Angew. Chem. Int. Ed*, Vol. 50, No. 13, 2011, pp. 2904-2939, <https://doi.org/10.1002/anie.201001374>.
- [20] N. Wang, H. Li, W. Lü, J. Li, J. Wang, Z. Zhang, Y. Liu, Effects of TiO<sub>2</sub> Nanotubes with Different Diameters on Gene Expression and Osseointegration of Implants in Minipigs, *Biomaterials*, Vol. 32, 2011, pp. 6900-6911, <https://doi.org/10.1016/j.biomaterials.2011.06.023>.
- [21] J. Kim, H. Lee, T. S. Jang, D. Kim, C. B. Yoon, G. Han, H. E. Kim, H. D. Jung, Characterization of Titanium Surface Modification Strategies for Osseointegration Enhancement, *Metals*, Vol. 11, No. 4, 2021, pp. 618, <https://doi.org/10.3390/met11040618>.
- [22] M. Curioni, The Behaviour of Magnesium During Free Corrosion and Potentiodynamic Polarization Investigated By Real-time Hydrogen Measurement and Optical Imaging, *Electrochim. Acta.*, Vol. 120, 2014, pp. 284-292, <https://doi.org/10.1016/j.electacta.2013.12.109>.

- [23] P. Bagheri, M. Farzam, A. B. Mousavi, M. Hosseini, Ni-TiO<sub>2</sub> Nanocomposite Coating with High Resistance to Corrosion and Wear. *Surf. Coat. Technol.*, Vol. 204, No. 23, 2010, pp. 3804-3810, <https://doi.org/10.1016/j.surfcoat.2010.04.061>.
- [24] S. Tiwari, R. Balasubramaniam, M. Gupta, Corrosion Behavior of SiC Reinforced Magnesium Composites, *Corros Sci*, Vol. 49, No. 2, 2007, pp. 711-725, <https://doi.org/10.1016/j.corsci.2006.05.047>.
- [25] A. Srivastava, R. Balasubramaniam, Electrochemical Impedance Spectroscopy Study of Surface Films Formed on Copper in Aqueous Environments, *Materials and Corrosion*, Vol. 56, No. 9, 2005, pp. 611-618, <https://doi.org/10.1002/maco.200503866>.
- [26] L. Li, Z. Zhang, L. Bo, Y. Cui, Y. Xu, Z. Zhang, In Situ Growth of TiO<sub>2</sub> nanotube Clusters, One-Step Octadecyl Self-Assembly and Its Corrosion Resistance, *Surf. Coat. Technol.*, Vol. 404, 2020, pp. 611-618, <https://doi.org/10.1016/j.surfcoat.2020.126470>.